



Published in final edited form as:

J Intell Mater Syst Struct. 2006 ; 17(7): 555–561.

Smart Rehabilitation Devices: Part II – Adaptive Motion Control

Shufang Dong¹, Ke-Qian Lu¹, J. Q. Sun^{1,*}, and Katherine Rudolph²

¹ Department of Mechanical Engineering, University of Delaware, Newark, DE 19716, USA

² Department of Physical Therapy, University of Delaware, Newark, DE 19716, USA

Abstract

This article presents a study of adaptive motion control of smart versatile rehabilitation devices using MR fluids. The device provides both isometric and isokinetic strength training and is reconfigurable for several human joints. Adaptive controls are developed to regulate resistance force based on the prescription of the therapist. Special consideration has been given to the human-machine interaction in the adaptive control that can modify the behavior of the device to account for strength gains or muscle fatigue of the human subject.

Keywords

muscle strengthening; smart rehabilitation device; magnetorheological fluids; smart materials for rehabilitation; adaptive control; motion tracking

INTRODUCTION

In Part 1 of this article, we introduced several prototypes of smart variable resistance exercise devices (VRED) for physical rehabilitation and discussed the force tracking control (Dong et al., 2005). In this article, we present the development of adaptive controls for regulating the joint motion of the patient during resistance exercises for muscle strengthening.

Muscle strengthening with resistance training has been reported to have positive effects on the recovery of normal physiological functions after neurological or traumatic injuries. A number of studies have shown that resistance training results in improved mobility, reduced pain, and improved stability of the elderly (Scarborough et al., 1999; Madsen et al., 2000) and of patients with knee osteoarthritis (OA) (Fisher et al., 1993) and rheumatoid arthritis (RA) (Vliet Vlieland, 2003). Resistance training also helps improve function in patients with impaired motor activity after stroke and in people with cerebral palsy (CP) (Teixeira-Salmela et al., 1999; Damiano et al., 2000; Dodd et al., 2002; Andrews and Bohannon, 2003). A common joint disorder, for which resistance exercise is often prescribed, is knee OA. It is estimated to occur in 10% of adults over 50 (Felson, 1990). Resistance exercise is an effective non-surgical intervention and is an important component of post-operative management following arthroscopic treatment or arthroplasty (Creamer and Hochberg, 1997). Studies of people with knee OA indicate that outcomes may be dependent on the mode of exercise (Topp et al., 2002; Huang et al., 2003): the isometric and isotonic exercises are suggested for relieving knee pain, and isokinetic exercise is recommended to increase joint stability and walking endurance. To reverse quadriceps weakness in patients after total knee arthroplasty, Stevens et al. (2003) suggested that resistance exercise with biofeedback may be necessary to facilitate muscle activation. Miyaguchi et al. (2003) found that isometric quadriceps resistance training results in reduced pain and improved function. They also found significant changes in the

*Author to whom correspondence should be addressed. E-mail: sun@me.udel.edu.

biochemistry of the knee-joint fluid, which may partially explain the analgesic effect of resistance exercise. Ide et al. (2003) found that resistance training can improve function in people with shoulder-joint instability.

The development of variable resistance devices reported in the previous article was motivated by the length–tension relationship of the skeletal muscle (Gordon et al., 1966). Muscle fibers change length with the joint angle. Therefore, the force-producing capacity of the muscle changes across the range of joint motion and is typically the highest in the mid range of joint motion. Muscle force generation during concentric exercise is also influenced by the contraction velocity (Hill, 1938). As the contraction velocity increases, the muscle force decreases. The force during isometric contraction when the muscle length does not change is higher than the force generated during concentric contraction. Therapists have hypothesized that optimal exercise for muscle strengthening should have a variable resistance profile through the range of joint motion that can maximize the strengthening effect without causing damages to muscle fibers. Current low-cost devices such as cuff weights and bar bells provide constant resistance through the entire range of joint motion, so exercise with such devices is not optimal.

The VRED is capable of regulating joint motion according to the needs of a particular patient. It takes muscle mechanics into consideration and adapts to the limb dynamics. In addition, to accurately regulate the resistance to provide isometric or variable resistance in response to dynamic muscle contractions, the control algorithms of the VRED can be developed to monitor the human–machine interaction in real-time and to provide visual feedback of the torque, joint motion, and velocity. Furthermore, the device can detect the dynamic characteristics of the patient, such as the muscle fatigue as well as the willingness to exercise, in order to modify the resistance during an exercise session. The device will allow the therapist to investigate therapeutic effects of prescribed exercise protocols in the patient’s own home. To realize all these intelligent functions of the VRED, we need a key element, i.e., an adaptive motion controller that can learn the dynamics of an individual patient in real-time, and change the device force output. It should be noted that in this article, we use the words force and torque interchangeably whenever the meaning is clear.

The article is organized as follows. The following discusses the MR damper, the human muscle force, and adaptive controls for joint motion regulation. Simulation and experimental results are presented in the subsequent section. The last section concludes the article.

MODELING AND CONTROL OF THE VRED

For a detailed description of the VRED, the readers are referred to Dong et al. (2005). Here, we focus on the modeling and adaptive control of the VRED.

We assume that the MR fluid and iron core of the electromagnetic coil operate in the lower linear range of the $B - H$ curve with the applied magnetic intensity far away from saturation. This assumption agrees with the conditions under which the rehabilitation exercise is carried out.

Plant Model

An RL circuit is used to model the MR damper coil (Vaughan and Gamble, 1996; Elmer and Gentle, 2001),

$$u = RI + L \frac{dI}{dt}, \quad (1)$$

where L is the self-inductance of the coil, R is the resistance of the coil, and u is the applied input voltage. Based on experimental observations, we assume that resistance R is slowly time-varying, since the damper temperature varies slightly during exercise, and that self-inductance L is also slowly time-varying.

Note that the human joint motion during exercise is a repetitive motion. For example, let x denote the knee angle. It is typically in the range $0^\circ < x < 135^\circ$ with $x = 0^\circ$ when the knee is straight. When the knee is flexed, $\dot{x} > 0$; when the knee extends, $\dot{x} < 0$. Since the resistance force is always against the motion, we shall only present the modeling and control design for the flexion when $\dot{x} > 0$.

The total resistive force of the MR damper is denoted as $f = f_\tau + f_\eta$. The off-state MR damper force f_η without the current input to the coil can be expressed as $f_\eta = c_1 + c_2\dot{x}$, where c_1 is a constant force due to static friction and $c_2\dot{x}$ is the viscous force. The on-state MR damper force f_τ is related to the current in the coil, the number of turns of the coil, the MR damper geometry, the magnetic flux cross area, and the magnetic induction curve of the material. Here, we adopt the approximation $f_\tau = c_3I$, where coefficient c_3 is slowly time-varying, and absorbs the effects of all the above factors. The total force of the MR damper becomes,

$$f = c_1 + c_2 \dot{x} + c_3 I (\dot{x} > 0). \quad (2)$$

Note that I is always positive in our electric circuit design. We assume that constant c_1 can be measured, and that c_2 and c_3 are unknown.

The dynamics of the human joint are usually described by a second-order quasi-linear system (Kearney and Hunter, 1990),

$$m \ddot{x} + c \dot{x} + kx = f_{\text{active}} - f (\dot{x} > 0), \quad (3)$$

where m represents the inertia of the limb, c represents the viscosity of the ligaments and articular surface, k is the elastic stiffness of the ligaments or due to cocontraction, and f_{active} denotes the contraction force of the muscle group.

We assume that contributions from passive viscosity c and stiffness k of the joint are negligible. There are many studies of the relationship between the muscle electromyographic (EMG) signal and resultant muscle force (Wang and Buchanan, 2002; Lloyd and Besier, 2003; Thelen, 2003). The complexity of the models makes it difficult to incorporate them into real-time controls with microprocessors. Here, we adopt a simple dynamic force model of the muscle as $f_{\text{active}} = \beta(t)h(x) - \alpha$, where $0 < \beta(t) \leq 1$, $\alpha > 0$, $h(x)$ is the isometric force profile, and $-\alpha$ describes the trend of decreasing muscle force with the increase in velocity (Dudley et al., 1990; Desplantez et al., 1999; Lee et al., 2000; Desplantez and Goubel, 2002). $\beta(t)$, known as the fatigue or intent coefficient, is a slowly varying parameter to compensate for the reduction of the isometric force after repeated contractions. Equation (3) now reads,

$$m \ddot{x} + \alpha \dot{x} - \beta(t)h(x) = -f (\dot{x} > 0). \quad (4)$$

Note that the isometric force profile $h(x)$ for a patient is measured before exercise as part of the evaluation of the patient by the physical therapist. It is hence a known function.

Adaptive Control

We consider the control design into three loops: the current loop, the force tracking, and the joint-motion regulation. The control architecture is illustrated in Figure 1. When designing a

control for an outer loop, we treat all the inner loops as ideal control systems such that they are stable with fast and accurate response to command inputs.

CURRENT LOOP—Define the coil current tracking error as $e_1 = I - I_d$, where I_d is the desired current level in the coil. Denote the estimate of the resistance R as \hat{R} and that of L as \hat{L} . The control voltage is given by

$$u = \hat{L}\dot{I}_d + \hat{R}I_d. \quad (5)$$

Substituting Equation (5) to Equation (1), we have

$$L\dot{e}_1 + Re_1 = \tilde{L}\dot{I}_d + \tilde{R}I_d, \quad (6)$$

where $\tilde{R} = \hat{R} - R$ and $\tilde{L} = \hat{L} - L$. Under the assumption that R and L are slowly time-varying, we propose the adaptive law to update the parameter estimation as (Slotine and Li, 1991)

$$\frac{d\hat{R}}{dt} = -\eta_1 e_1 I_d, \quad \frac{d\hat{L}}{dt} = -\eta_2 e_1 \dot{I}_d, \quad (7)$$

where η_1 and η_2 are positive adaptation gains.

Consider a Lyapunov function $V_1(e_1) = (1/2)e_1^2 + (1/2\eta_1 L)\tilde{R}^2 + (1/2\eta_2 L)\tilde{L}^2$.

$$\begin{aligned} \dot{V}_1 &= e_1 \dot{e}_1 + \frac{1}{\eta_1 L} \tilde{R} \frac{d\tilde{R}}{dt} + \frac{1}{\eta_2 L} \tilde{L} \frac{d\tilde{L}}{dt} \\ &= -\frac{R}{L} e_1^2 + \frac{1}{L} e_1 (\tilde{L} \dot{I}_d + \tilde{R} I_d) \\ &\quad + \frac{1}{\eta_1 L} \tilde{R} (-\eta_1 e_1 I_d) + \frac{1}{\eta_2 L} \tilde{L} (-\eta_2 e_1 \dot{I}_d) \\ &= -\frac{R}{L} e_1^2 < 0. \end{aligned} \quad (8)$$

According to the invariant set theorem (Slotine and Li, 1991), the closed loop current system is stable and the current tracking error e_1 will converge to zero as $t \rightarrow \infty$.

RESISTIVE FORCE TRACKING—We assume that the closed loop RL network is an ideal current source. To account for the slowly timevarying and uncertain coefficients c_2 and c_3 of the damper force in Equation (2), we consider an adaptive control for force tracking.

Let \hat{c}_2 and \hat{c}_3 denote the estimated values of c_2 and c_3 . The desired resistive force is f_r . The control current for the force tracking is given by

$$I = \frac{f_r - c_1 - \hat{c}_2 \dot{x}}{\hat{c}_3} (\dot{x} > 0). \quad (9)$$

We denote the force tracking error as $e_f = f_r - f$. Substituting control I in Equation (2), we have

$$e_f = \tilde{c}_2 \dot{x} + \tilde{c}_3 I, \quad (10)$$

where the parameter estimation errors are $\tilde{c}_2 = \hat{c}_2 - c_2$ and $\tilde{c}_3 = \hat{c}_3 - c_3$.

Similarly, we propose the adaptive law to update the parameter estimation as

$$\frac{d\hat{c}_2}{dt} = -\gamma_2 e_f \dot{x}, \quad \frac{d\hat{c}_3}{dt} = -\gamma_3 e_f I, \quad (11)$$

where γ_2 and γ_3 are positive adaptation gains. Consider another Lyapunov function $V_f = (\tilde{c}_2^2/2\gamma_2) + (\tilde{c}_3^2/2\gamma_3)$.

$$\begin{aligned}\dot{V}_f &= \frac{\tilde{c}_2}{\gamma_2} \frac{d\tilde{c}_2}{dt} + \frac{\tilde{c}_3}{\gamma_3} \frac{d\tilde{c}_3}{dt} \\ &= -\frac{c_2\gamma_2 e_f \dot{x}}{\gamma_2} - \frac{c_3\gamma_3 e_f \dot{x}}{\gamma_3} \\ &= -e_f(c_2 \dot{x} + c_3 I) = -e_f^2 > 0.\end{aligned}\quad (12)$$

According to the invariant set theorem (Slotine and Li, 1991), the force tracking error $e_f \rightarrow 0$ as $t \rightarrow \infty$.

MOTION REGULATION—Let us proceed to the adaptive control design for motion regulation assuming that the force controller delivers the desired force level quickly and accurately. Let $x_r(t)$ be the desired motion profile and the motion tracking error be $e = x - x_r$. Define a sliding function $s = \dot{e} + \lambda e$, where $\lambda > 0$. Let \hat{m} , $\hat{\alpha}$ and $\hat{\beta}$ be the estimates of m , α , and β , respectively. Going through the steps of sliding mode control (Slotine and Li, 1991), we arrive at a control force as

$$f = -\hat{m}(\dot{x}_r - \lambda \dot{e}) - \hat{\alpha} \dot{x} + \hat{\beta} h(x) + ks(\dot{x} > 0), \quad (13)$$

where $k > 0$ is a control gain. Substituting the control to Equation (4), we have

$$m \dot{s} + ks = \tilde{m}(\dot{x}_r - \lambda \dot{e}) + \tilde{\alpha} \dot{x} + \tilde{\beta}(-h(x)), \quad (14)$$

where $\tilde{m} = \hat{m} - m$, $\tilde{\alpha} = \hat{\alpha} - \alpha$, and $\tilde{\beta} = \hat{\beta} - \beta$

We would like the parameter estimates to converge to the true values of corresponding parameters. To achieve this, we apply the composite adaptation law. To prepare for this, we first multiply both sides of Equation (4) by $\lambda_f/(p) + \lambda_f$, where p is the Laplace variable and $\lambda_f > 0$ is a constant. In real-time implementation, the quantity multiplied by this factor is passed through a low-pass filter with bandwidth λ_f . We yield

$$mv_1 + \alpha v_2 + \beta v_3 = w, \quad (15)$$

where

$$\begin{aligned}v_1 &= \frac{\lambda_f p}{p + \lambda_f} \dot{x}, & v_2 &= \frac{\lambda_f}{p + \lambda_f} \dot{x}, \\ v_3 &= \frac{\lambda_f}{p + \lambda_f} (-h(x)), & w &= \frac{\lambda_f}{p + \lambda_f} (-f).\end{aligned}\quad (16)$$

Define the predicted value of w as $\hat{w} = m\hat{c}v_1 + \hat{\alpha}v_2 + \hat{\beta}v_3$. The prediction error e_w is

$$e_w = \hat{w} - w = \tilde{m} v_1 + \tilde{\alpha} v_2 + \tilde{\beta} v_3. \quad (17)$$

Introduce the vectors $\Theta = [m, \alpha, \beta]^T$, $\hat{\Theta} = [m\hat{c}, \hat{\alpha}, \hat{\beta}]^T$, $\tilde{\Theta} = \hat{\Theta} - \Theta$, $\mathbf{U}_s = [(\dot{x}_r - \lambda \dot{e}), \dot{x}, (-h(x))]^T$. Equations (14) and (17) are reduced to

$$\dot{s} = -\frac{k}{m} s + \frac{1}{m} \tilde{\Theta}^T \mathbf{U}_s, \quad (18)$$

$$e_w = \tilde{\Theta}^T \mathbf{U}. \quad (19)$$

Combining the adaptation for motion tracking and for parameter estimation, we obtain the composite adaptation law as

$$\frac{d\hat{\Theta}}{dt} = -\mathbf{P}[s\mathbf{U}_s + \xi(t)e_w\mathbf{U}], \quad (20)$$

where $\xi(t) > 1/2$ is a weight to balance the effect of tracking error and prediction error, and \mathbf{P} is a symmetric positive definite gain matrix updated by the following equation, according to the exponentially forgetting algorithm (Slotine and Li, 1991)

$$\frac{d}{dt}[\mathbf{P}] = \phi(t)\mathbf{P} - \mathbf{P}\mathbf{U}\mathbf{U}^T\mathbf{P}, \quad (21)$$

$$\frac{d}{dt}[\mathbf{P}^{-1}] = -\phi(t)\mathbf{P}^{-1} + \mathbf{U}\mathbf{U}^T, \quad (22)$$

where $\phi(t) > 0$ is a forgetting factor.

Consider a Lyapunov function $V = (1/2)[s^2 + (1/m) \times \tilde{\Theta}^T \mathbf{P}^{-1} \tilde{\Theta}]$. We have

$$\begin{aligned} \dot{V} &= \frac{1}{2} \left\{ 2s \dot{s} + \frac{2}{m} \tilde{\Theta}^T \mathbf{P}^{-1} \frac{d\tilde{\Theta}}{dt} + \frac{1}{m} \tilde{\Theta}^T \frac{d}{dt}[\mathbf{P}^{-1}] \tilde{\Theta} \right\} \\ &= -\frac{k}{m} s^2 - \frac{\phi(t)}{2m} \tilde{\Theta}^T \mathbf{P}^{-1} \tilde{\Theta} - \frac{\xi(t) - (1/2)}{m} e_w^2 < 0. \end{aligned} \quad (23)$$

Hence, the system is stable. When $\dot{V} = 0$, we must have $s = 0$, $e_w = 0$, and $\tilde{\Theta} = 0$. According to the invariant set theorem (Slotine and Li, 1991), the motion tracking error e and prediction error e_w will converge to zero, and the estimated parameters will converge to their true values.

SIMULATION AND EXPERIMENTAL RESULTS

Before we present the simulation and experimental results, we first discuss the hardware and its limitations. The DC voltage for the MR damper is 0–12 V. The amplifier for the digital controller has a dead zone of 0.2V and is slightly nonlinear. We model the amplifier by a linear relationship $u = 5.56(u_c - 0.2)$ based on experimental data where $u > 0$ is the applied voltage, and u_c is the corresponding digital command. The current I is measured through the voltage across a 1 Ω resistor in series with the coil of the damper. The resistive force and flexion angle reading of the VRED are carefully calibrated.

The angular velocity of the joint is obtained by differentiating a low-pass filtered angle measurement with 5Hz cut-off frequency. The digital version of the velocity expression is given by

$$\dot{x}_n = 0.8834\dot{x}_{n-1} + 31(x_n - x_{n-1}). \quad (24)$$

The sample frequency of the digital controller is 250 Hz.

The nominal parameters for simulations are as follows: $c_1 = 15$, $c_2 = 9$, $c_3 = 100$, $R = 7.5$) $2 \cos(4t)$, $L = 0.15 + 0.05 \sin(4t)$, $\alpha = 10$, $\beta = 1$, $m = 4$ and $h(x) = 100 + 30 \sin(10x)$. In both simulations and experiments, adaptive gains are $\eta_1 = 500$, $\eta_2 = 10$, $\gamma_2 = 10$, $\gamma_3 = 150$ and $k = 30$. The low-pass filter gains are $\lambda = 1$, $\lambda_f = 20$ and $\phi(t) = 1$. The composite adaptation weight $\zeta(t) = 1$. The initial values for the adaptive control in simulations are $\hat{R} = 7.5$, $\hat{L} = 0.15$, $\hat{m} = 6$, $\hat{\alpha} = 9$, $\hat{\beta} = 1.1$, $\hat{c}_1 = 15$, $\hat{c}_2 = 6$, and $\hat{c}_3 = 80$. These values are the same for the experiments except for $\hat{\alpha} = 30$ and $\hat{\beta} = 1$. The initial value of the gain matrix \mathbf{P} is $[100, 0, 0; 0, 50, 0; 0, 0, 0.1]$.

Figure 2 shows the simulated coil current tracking. Figure 3 shows the simulated damper force tracking. Figure 4 shows the motion regulation together with the online parameter estimation. The current and force loops perform fast and accurately. The motion control shows good regulation. The online parameter estimation converges quickly. Note that it is common in the physical therapy community to express results in terms of the joint angle. Hence, the joint angle is used in the figures showing the force and motion regulations.

The experimental result of the adaptive current control is shown in Figure 5. The performance is better than that in the simulation because nominal values of inductance and resistance of the electromagnetic coil are much more oscillatory in the simulation than in the experiment.

In the force and motion control experiments, a healthy male adult is the subject. The experimental results of force tracking are shown in Figure 6. The force tracking is fast and accurate with a small overshoot near the beginning. This may be attributed to the time-delay of the system. Figure 7 shows the experimental results of the motion regulation of the knee joint. The muscle force parameters are dynamically predicted online. The experiments are very satisfactory indeed.

In summary, we have demonstrated the effectiveness of the adaptive controls with a set of chosen control gains and parameters and a limited test on one human subject. Investigations on the effect of control gains and parameters and the control performance with a diverse group of patients will be carried out in the future.

CONCLUSIONS

We have presented a study of adaptive motion control of a versatile rehabilitation device with MR dampers. The coupled model of the human joint and the device is proposed for the control design. The adaptive control regulates the resistive force of the damper while attaining the prescribed joint motion profile, effectively deals with uncertainties of the system, and achieves excellent force- and motion-tracking performance. The VRED will be evaluated in a clinical setting. Its rehabilitation effectiveness on various patients will be studied in the near future.

Acknowledgements

This work is supported by a grant (5 R21 HD040956-03) from the National Institute of Health.

References

- Andrews AW, Bohannon RW. Short-term Recovery of Limb Muscle Strength after Acute Stroke. *Archives of Physical Medicine and Rehabilitation* 2003;84(1):125–130. [PubMed: 12589633]
- Creamer P, Hochberg MC. Osteoarthritis. *Lancet* 1997;350(9076):503–509. [PubMed: 9274595]
- Damiano DL, Martellotta TL, Sullivan DJ, Granata KP, Abel MF. Muscle Force Production and Functional Performance in Spastic Cerebral Palsy: Relationship of Cocontraction. *Archives of Physical Medicine and Rehabilitation* 2000;81(7):895–900. [PubMed: 10896001]
- Desplantez A, Goubel F. *In vivo* Force-velocity Relation of Human Muscle: A Modelling from Sinusoidal Oscillation Behaviour. *Journal of Biomechanics* 2002;35(12):1565–1573. [PubMed: 12445609]
- Desplantez A, Cornu C, Goubel F. Viscous Properties of Human Muscle during Contraction. *Journal of Biomechanics* 1999;32(1):555–562. [PubMed: 10332618]
- Dodd KJ, Taylor NF, Damiano DL. A Systematic Review of the Effectiveness of Strength-training Programs for People with Cerebral Palsy. *Archives of Physical Medicine and Rehabilitation* 2002;83(8):1157–1164. [PubMed: 12161840]
- Dong S, Lu K-Q, Sun JQ, Rudolph K. Smart Rehabilitation Devices – Part 1. Force Tracking Control. *Journal of Intelligent Material Systems and Structures*. 2005(in press)

- Dudley GA, Harris RT, Duvoisin MR, Hather BM, Buchanan P. Effect of Voluntary vs. Artificial Activation Torque (Nm) on the Relationship of Muscle Torque to Speed. *Journal of Applied Physiology* 1990;69(6):2215–2221. [PubMed: 2077019]
- Elmer KF, Gentle CR. A Parsimonious Model for the Proportional Control Valve. *Proceedings of the Institution of Mechanical Engineers – Part C* 2001;215(11):1357–1363.
- Felson D. The Epidemiology of Knee Osteoarthritis. *Seminars in Arthritis and Rheumatism* 1990;20(3 supplement 1):42–50. [PubMed: 2287948]
- Fisher NM, Gresham GE, Abrams M, Hicks J, Horrigan D, Pendergast DR. Quantitative Effects of Physical Therapy on Muscular and Functional Performance in Subjects with Osteoarthritis of the Knees. *Archives of Physical Medicine and Rehabilitation* 1993;74(8):840–847. [PubMed: 8347069]
- Gordon AM, Huxley AF, Julian FJ. The Variation in Isometric Tension with Sarcomere Length in Vertebrate Muscle Fibres. *Journal of Physiology* 1966;184:170–192. [PubMed: 5921536]
- Hill AV. The Heat of Shortening and the Dynamic Constants of Muscle. *Proceedings of Royal Society of London Series B* 1938;B126:136–195.
- Huang M-H, Lin Y-S, Yang R-C, Lee C-L. A Comparison of Various Therapeutic Exercise on the Functional Status of Patients with Knee Osteoarthritis. *Seminars in Arthritis and Rheumatism* 2003;32(6):398–406. [PubMed: 12833248]
- Ide J, Maeda S, Yamaga M, Morisawa K, Takagi K. Shoulder-strengthening Exercise with an Orthosis for Multidirectional Shoulder Instability: Quantitative Evaluation of Rotational Shoulder Strength Before and After the Exercise Program. *Journal of Shoulder and Elbow Surgery* 2003;12(4):342–345. [PubMed: 12934027]
- Kearney RE, Hunter IW. System Identification of Human Joint Dynamics. *Critical Reviews in Biomedical Engineering* 1990;18(1):55–87. [PubMed: 2204515]
- Lee H-D, Suter E, Herzog W. Effects of Speed and Distance of Muscle Shortening on Force Depression during Voluntary Contractions. *Journal of Biomechanics* 2000;33(8):917–923. [PubMed: 10828321]
- Lloyd DG, Besier TF. An EMG-driven Musculoskeletal Model to Estimate Muscle Forces and Knee Joint Moments *in vivo*. *Journal of Biomechanics* 2003;36(6):765–776. [PubMed: 12742444]
- Madsen OR, Lauridsen UB, Sorensen OH. Quadriceps Strength in Women with a Previous Hip Fracture: Relationships to Physical Ability and Bone Mass. *Scandinavian Journal of Rehabilitation Medicine* 2000;32(1):37–40. [PubMed: 10782940]
- Miyaguchi M, Kobayashi A, Kadoya Y, Ohashi H, Yamano Y. Biochemical Change in Joint Fluid after Isometric Quadriceps Exercise for Patients with Osteoarthritis of the Knee. *Osteoarthritis and Cartilage* 2003;11(4):252–259. [PubMed: 12681951]
- Scarborough DM, Krebs DE, Harris BA. Quadriceps Muscle Strength and Dynamic Stability in Elderly Persons. *Gait & Posture* 1999;10(1):10–20. [PubMed: 10469937]
- Slotine, J-JE.; Li, W. *Applied Nonlinear Control*. Prentice Hall; Englewood Cliffs, New Jersey: 1991.
- Stevens JE, Mizner RL, Snyder-Mackler L. Quadriceps Strength and Volitional Activation Before and After Total Knee Arthroplasty for Osteoarthritis. *Journal of Orthopaedic Research* 2003;21(5):775–779. [PubMed: 12919862]
- Teixeira-Salmela LF, Olney SJ, Nadeau S, Brouwer B. Muscle Strengthening and Physical Conditioning to Reduce Impairment and Disability in Chronic Stroke Survivors. *Archives of Physical Medicine and Rehabilitation* 1999;80(10):1211–1218. [PubMed: 10527076]
- Thelen DG. Adjustment of Muscle Mechanics Model Parameters to Simulate Dynamic Contractions in Older Adults. *Journal of Biomechanical Engineering* 2003;125(1):70–77. [PubMed: 12661198]
- Topp R, Woolley S, Hornyak J, Khuder S, Kahaleh B. The Effect of Dynamic versus Isometric Resistance Training on Pain and Functioning among Adults with Osteoarthritis of the Knee. *Archives of Physical Medicine and Rehabilitation* 2002;83(9):1187–1195. [PubMed: 12235596]
- Vaughan ND, Gamble JB. The Modeling and Simulation of a Proportional Solenoid Valve. *Journal of Dynamic Systems, Measurement, and Control* 1996;118(3):120–125.
- Vliet Vlieland TPM. Rehabilitation of People with Rheumatoid Arthritis. *Best Practice & Research Clinical Rheumatology* 2003;17(5):847–861. [PubMed: 12915161]
- Wang L, Buchanan TS. Prediction of Joint Moments using a Neural Network Model of Muscle Activations from EMG Signals. *IEEE Transactions on Neural Systems and Rehabilitation Engineering* 2002;10(1):30–37. [PubMed: 12173737]

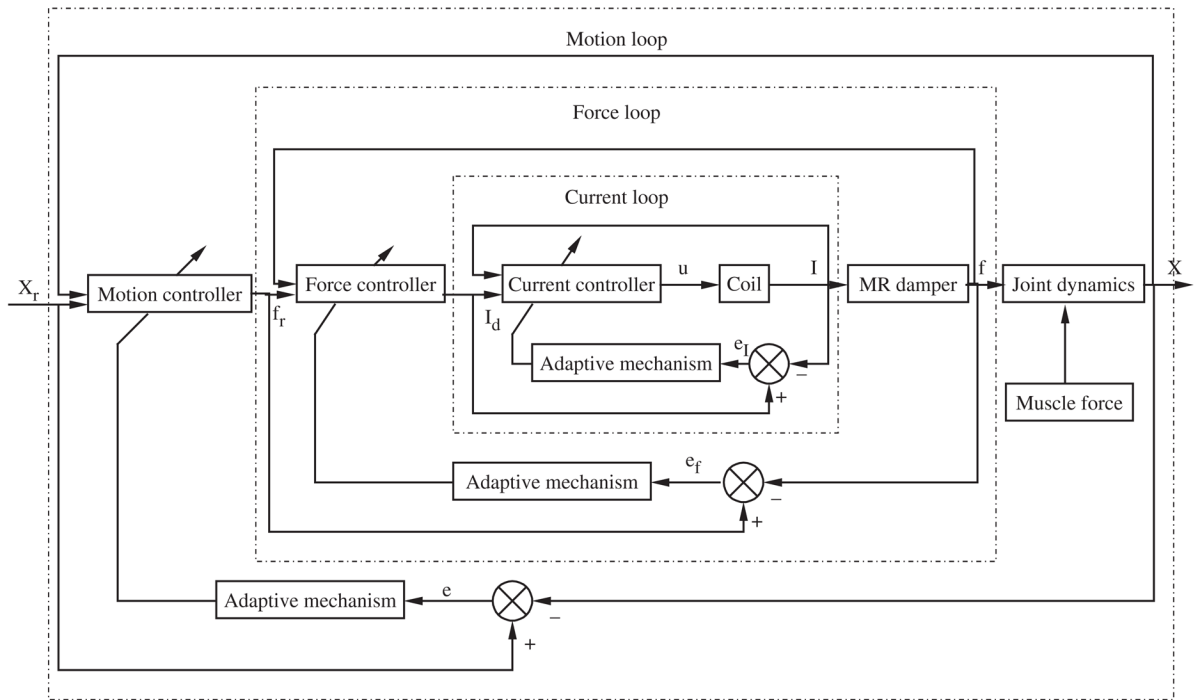


Figure 1. Configuration of the control system for the versatile rehabilitation device.

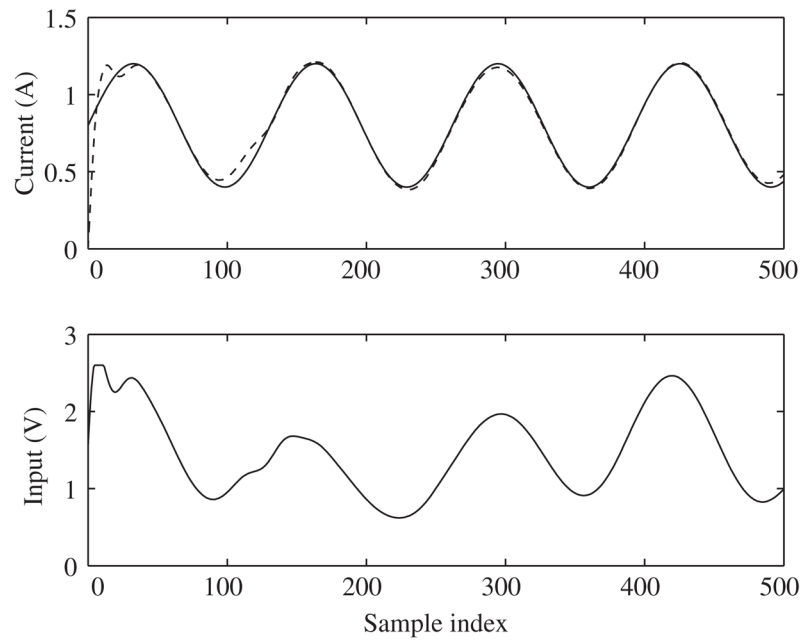


Figure 2. Simulation of the adaptive current control. Solid line: The reference. Dashed line: The actual current.

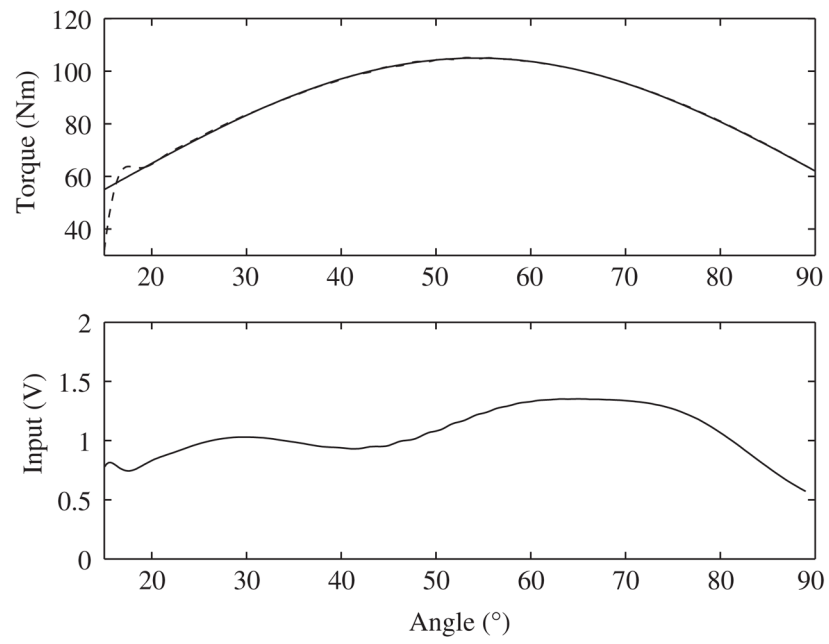


Figure 3. Simulation of the adaptive force control. Top: The torque tracking. Solid line: The desired force. Dashed line: The actual torque. Bottom: The coil voltage input.

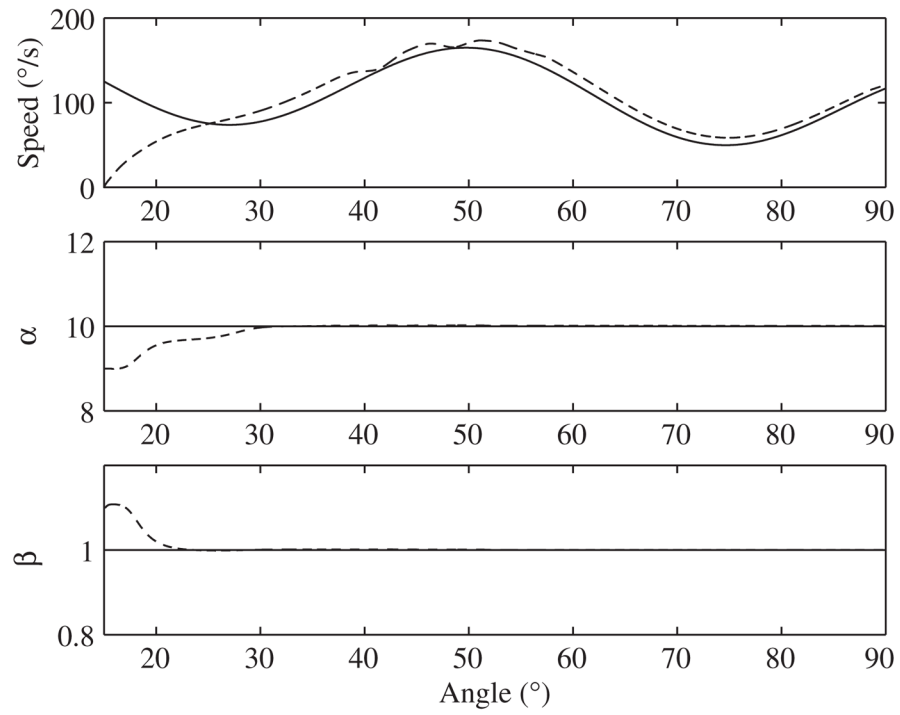


Figure 4. Simulation of the adaptive joint motion regulation. Solid line: The prescribed motion profile or the true parameters. Dashed line: The actual motion or the estimated parameters.

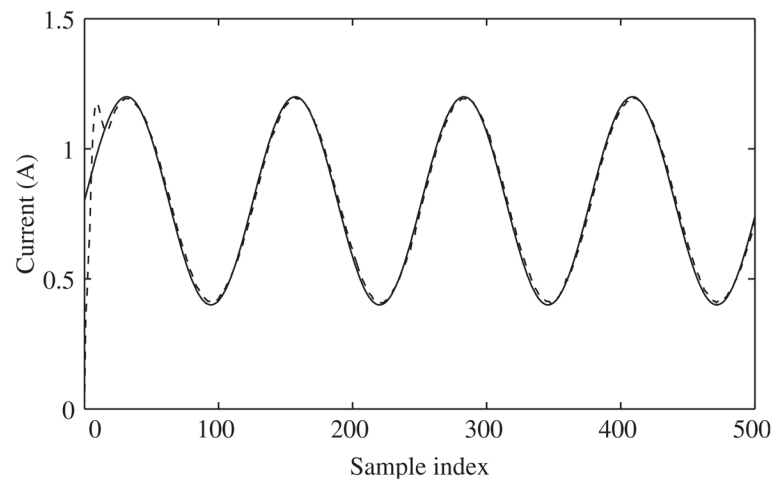


Figure 5. Experimental results of the adaptive current control. Solid line: The reference. Dashed line: The actual current output. This figure compares well with Figure 2.

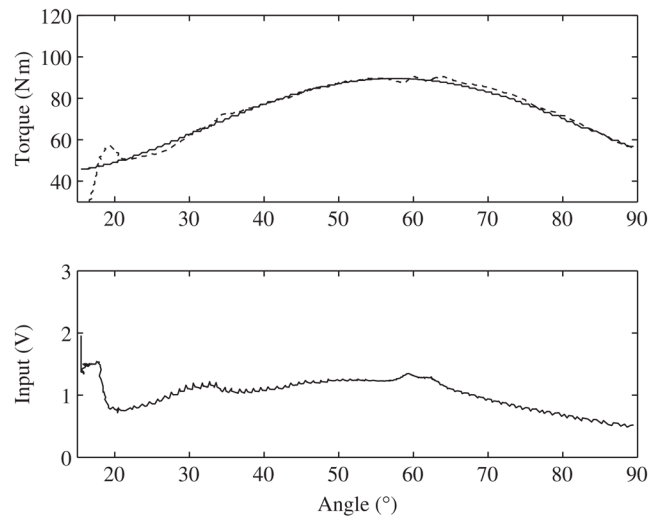


Figure 6. Experimental results of the adaptive force control. Top: The force tracking. Solid line: The desired force. Dashed line: The actual force. Bottom: The coil voltage input.

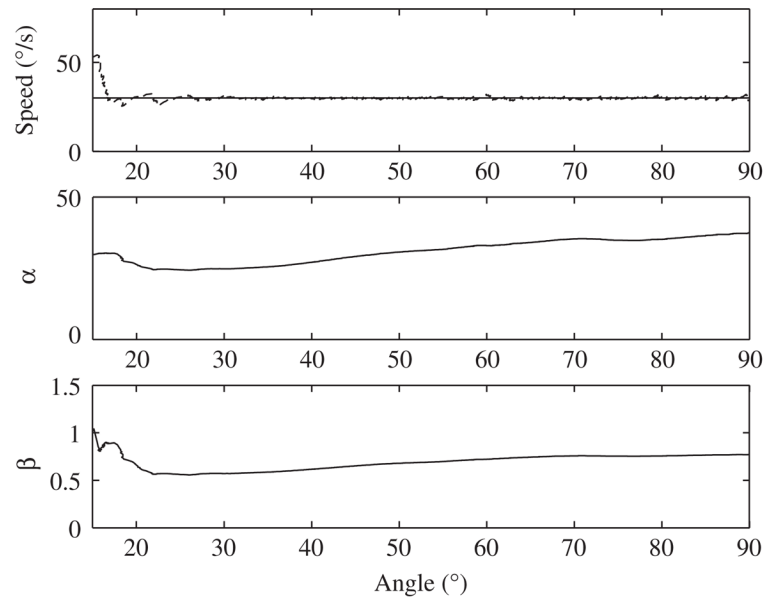


Figure 7. Experimental results of the knee joint motion regulation and parameter estimations. In the top figure, Solid line: The prescribed joint speed. Dashed line: The actual speed.